IoT-Integrated Gas Sensing for Battery Management Systems in Electric Vehicles: A Review on Progress, Challenges, and Future Research

Amogh Anil Sambare
Deen Dayal Upadhyay Kaushal Kendra, Automobile Division,
Dr. Babasaheb Ambedkar Marathwada University, Chhatrapati Sambhajinagar,
Maharashtra 431004, India

Abstract

The rapid electrification of road transport has placed battery management systems (BMS) at a critical interface between operational performance and safety. Lithium-ion batteries (LIBs) used in electric vehicles (EVs) are susceptible to catastrophic failure modes, particularly thermal runaway, accompanied by the emission of toxic and flammable gases such as carbon monoxide (CO), hydrogen fluoride (HF), hydrogen (H_2), methane (CH_4), and volatile organic compounds (VOCs). The early detection of these gases through integrated sensing strategies offers an important pathway for preventing fires, explosions, and loss of life. This review critically examines the convergence of Internet of Things (IoT) technologies with advanced gas-sensing modalities to build intelligent, proactive BMS architectures. We systematically reviewed the electrochemical mechanisms of gas generation in lithium-ion cells under abuse and degradation conditions, classified gas sensor technologies applicable to EV battery packs, including metal oxide semiconductors, electrochemical sensors, optical sensors, and nanomaterial-based platforms, and analyzed their integration with IoT frameworks, encompassing IoT hardware, edge computing, and machine learning algorithms. Comparative tables synthesize the sensing performance, deployment suitability, and intelligent processing pipelines of these platforms. Prominent challenges, including sensor cross-sensitivity, packaging constraints, data latency, cybersecurity, and regulatory gaps, have been identified. This review concludes by mapping emerging research directions, such as multi-gas sensor fusion, large language model-assisted diagnostics, digital twin integration, and solid-state battery-compatible sensing, providing a roadmap for fail-safe, self-aware EV battery systems.

Keywords: *Battery management system, Gas sensor, Thermal runaway, Electric vehicle, IoT, Machine learning, Lithium-ion battery, Early warning system, Edge computing, Sensor fusion*

1. Introduction

The global adoption of EVs has accelerated significantly over the past decade. This growth has been driven by climate policies, rising battery energy densities, and decreasing manufacturing costs. By 2023, over 40 million EVs were on the roads worldwide [1]. The national decarbonization targets project that this figure will exceed 300 million by 2035. All battery electric vehicles depend on lithium-ion battery packs. These packs must deliver high energy and power densities to be effective.

* Corresponding author. Tel.: +91-9420056178;
E-mail address: asambare.ddukk@bamu.ac.in

Manuscript History:
Received 16 June, 2026, Revised 22 September, 2026, Accepted 30 September, 2026, Published 31 October, 2026
Copyright © 2026 UNIMAS Publisher. This is an open access article under the CC BY-NC-SA 4.0 license.
https://doi.org/10.33736/jaspe.13432.2026

e-ISSN: 2289-7771

They must also meet strict safety requirements under thermal, mechanical, and electrochemical conditions.

Lithium-ion batteries carry inherent risks owing to their reactive electrolytes and electrode chemistries. The most serious failure mode is thermal runaway. Internal short circuits, overcharging, external heating, and mechanical damage can trigger these reactions. Once triggered, a self-sustaining exothermic reaction produces a fire or an explosion [1,2]. Before thermal runaway, the degrading cells release specific gases. Carbon monoxide, hydrogen, methane, ethylene, acetylene, dimethyl carbonate vapor, and hydrogen fluoride can be detected sequentially. Each gas corresponds to a generalized stage of cell deterioration [3-5]. Together, they form a readable chemical signature of the cell condition.

Conventional BMS designs track the voltage, current, and temperatures. From these, they estimate the state of charge (SoC) and state of health (SoH) of the battery. The problem is timing. In large automotive packs, cell-level faults can be electrically invisible at the pack level [6]. By the time pack-level changes appear, the fault may become irreversible. Gas sensors inside battery enclosures detect vented gases three to eight minutes earlier, providing a critical warning window between the initial cell venting event and pack-level thermal runaway propagation. This window precedes any measurable voltage or temperature shifts [7,8,10]. Three to eight minutes is sufficient time to isolate the modules or alert the driver.

Raw gas readings alone are insufficient for reliable fault classification. A carbon monoxide spike from normal aging appears different from that preceding cell venting. The distinction between these gases requires simultaneous pattern recognition across several gas channels. This is where the IoT architecture becomes relevant, as shown in Figure 1. Edge processors run convolutional and recurrent models directly on the vehicles. They classify gas data in real time without cloud round trips [9]. Cloud latency, often several seconds, is too slow when the event window is minutes wide.

This study addresses this problem. Section 2 covers the electrochemistry of gas generation in lithium-ion batteries. Section 3 reviews the sensor technologies against automotive deployment constraints. Section 4 examines IoT hardware, communication protocols, and AI inference methods. Section 5 maps open problems: cross-sensitivity, packaging under vibration and heat, cybersecurity exposure, and missing standards. Section 6 proposes future research directions. The intended readers are researchers, BMS engineers, and safety regulators.

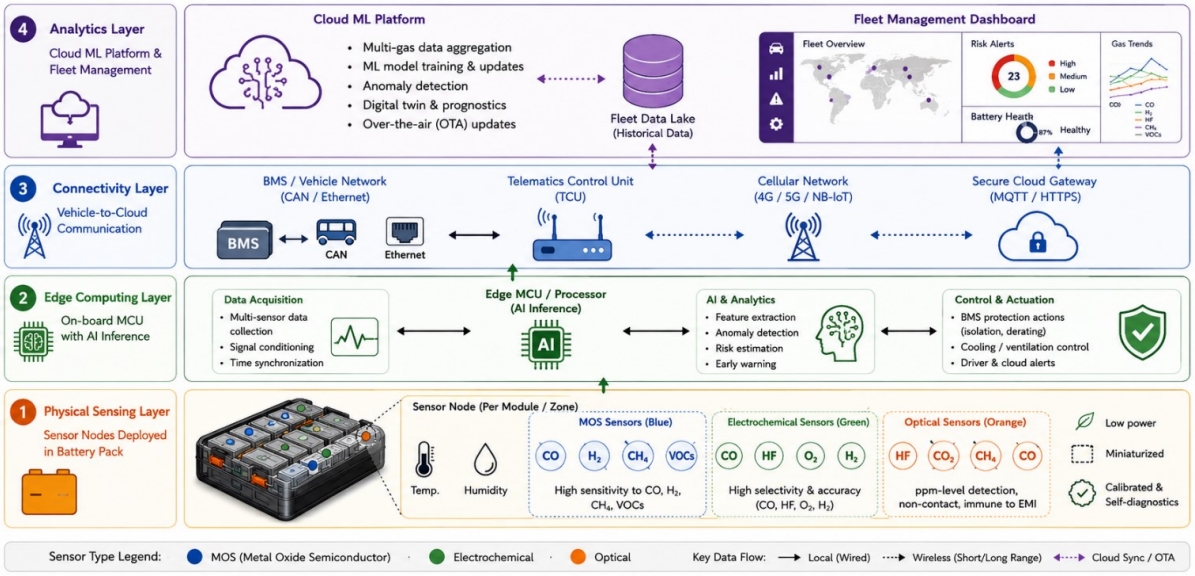


Figure 1. Schematic overview of the IoT-integrated BMS gas monitoring architecture

2. Electrochemical basis of gas generation in lithium-ion batteries

2.1. Normal operation and solid electrolyte interphase formation

During the early cycles, the electrolyte solvents decompose electrochemically at the anode. The solvents used are typically ethylene carbonate (EC) and dimethyl carbonate (DMC). This decomposition forms a protective layer known as the solid electrolyte interphase (SEI). The SEI allows the passage of lithium ions while blocking further electrolyte degradation. This is essential for stable, long-term cell operation. The formation of the SEI releases small amounts of gas. CO_2, CO, CH_4, C_2H_4, and H_2 are the principal gases produced, as shown in Figure 2 [19,23]. Most of these gases remain trapped inside the cells during the early cycles. They accumulate and escape under three conditions: SEI instability, physical cell damage, and temperature increase. Gas generation does not cease after the initial cycles. The SEI continues to grow and repair itself over hundreds of charge–discharge cycles. Films are also formed on the cathode surface over time. At high charge rates, Li plating occurs on the anodes. Each of these processes adds gas to the cells.

2.2. Adverse conditions and pre-thermal-runaway outgassing

Overcharging, over-discharge, external heating, and mechanical deformation significantly accelerate gas generation. Each abuse condition triggers distinct electrochemical reactions within the cells. Overcharging pushes the cathode voltage beyond its upper limit. This drives the oxidation of the electrolyte at the cathode surface. Delithiated transition metal oxides, particularly in NMC and NCA chemistries, release O_2. O_2 reacts exothermically with organic electrolytes. The products of this reaction are CO_2, CO, and water vapor [16,22]. Thermal abuse follows a temperature-dependent sequence. Between 80 and 130°C, the SEI decomposition releases CO_2 and CO. Above 130°C, the separator melts, and internal short circuits are formed. These short circuits generate rapid Joule heating. At 150–180°C, anode-electrolyte reactions produce H_2 and hydrocarbons. Beyond 200°C, the cathode structure collapses and releases O_2. O_2 drives the combustion process. Flammable and toxic gases are then vented at high pressures [2,12,13]. This outgassing sequence has been experimentally characterized. Researchers have used gas chromatography–mass spectrometry (GC-MS) and ion chromatography to study this. The data were obtained from controlled thermal runaway experiments [4-6,8]. Among the gases produced, hydrogen fluoride (HF) is the most hazardous. $LiPF_6$ salt decomposes in the presence of moisture and heat to form HF. Even part-per-million concentrations are acutely toxic to humans. HF is corrosive to metal and polymer sensor components [6,7]. Therefore, it threatens both occupant safety and sensor durability.

2.3. Gas signature analysis and its diagnostic value

The gas release kinetics were quantified using commercial 18650 format cells. CO generation begins 8–15 min before any measurable increase in the cell surface temperature [11]. This early window is specifically applicable to heating-induced thermal runaway scenarios. H_2 appeared slightly later than did CO. Its concentration increased steeply and correlated with the rate of thermal acceleration. VOC species appear even earlier than CO. Dimethyl carbonate vapor and diethyl carbonate are detectable at relatively low temperatures [17-18,65]. Their presence indicates electrolyte evaporation before the thermal abuse threshold is reached. These findings have direct and practical implications. The chemical signatures preceded the thermal signatures by a few minutes. Therefore, gas sensing can function as an early warning system in BMS architectures. It detects fault conditions before the voltage and temperature sensors respond. Table 1 summarizes the key gas species relevant to EV battery monitoring. Each species is listed alongside its primary generation mechanism, onset temperature, and target concentration range.

2.4. Influence of battery chemistry and cell-to-pack architecture on gas evolution and detection

The gas-generation behavior and thermal characteristics of lithium-ion batteries vary significantly with cell chemistry. High-nickel NMC/NCA batteries generally exhibit higher heat-release rates, greater oxygen evolution, and faster thermal-runaway propagation than LFP/LMFP batteries, resulting in more rapid increases in CO, H_2, and VOC concentrations. In contrast, LFP/LMFP chemistries typically demonstrate lower heat release and improved thermal stability, although combustible gases are still generated during failure events. The adoption of Cell-to-Pack (CTP) architectures further influences gas-detection performance by reducing module-level headspace and altering gas-flow pathways within the battery enclosure. Liquid-cooling channels and pack geometry can significantly affect gas dispersion, sensor response latency, and local gas accumulation, making sensor placement a critical design consideration. Consequently, computational fluid dynamics (CFD)-based optimization of sensor locations is increasingly recommended to ensure reliable and timely detection of vent gases in modern CTP battery packs.

Table 1. Key gas species generated by lithium-ion battery failure, their sources, onset temperatures, and detection targets

Gas Species	Primary Source	Onset Temp. (°C)	Target Conc. Range (ppm)	Health/Safety Limit	Reference
Carbon Monoxide (CO)	Electrolyte decomposition, SEI breakdown	80–120	50–1000	25 ppm TWA (OSHA)	[4,6]
Hydrogen (H_2)	Anode–electrolyte reaction, overcharge	100–150	100–10,000	4% LFL (flammable)	[5,6]
Hydrogen Fluoride (HF)	LiPF6 hydrolysis, cathode decomposition	100–160	1–50	0.5 ppm ceiling (NIOSH)	[6]
Methane (CH_4)	Electrolyte reduction at anode	130–200	50–5000	5% LFL (flammable)	[8,17]
Ethylene (C_2H_4)	EC reduction by-product	80–130	20–500	Flammable (2.7% LFL)	[11]
Carbon Dioxide (CO_2)	SEI formation, carbonate oxidation	60–100	500–50,000	5000 ppm STEL	[17,4,6]
Dimethyl Carbonate (DMC)	Electrolyte evaporation / combustion	40–80	10–200	Threshold odor ~4 ppm	[24,27]
Acetylene (C_2H_2)	High-temp. electrolyte pyrolysis	180–250	1–100	Flammable (2.5% LFL)	[29,30]

LFL, lower flammable limit; TWA, time-weighted average; STEL, short-term exposure limit.

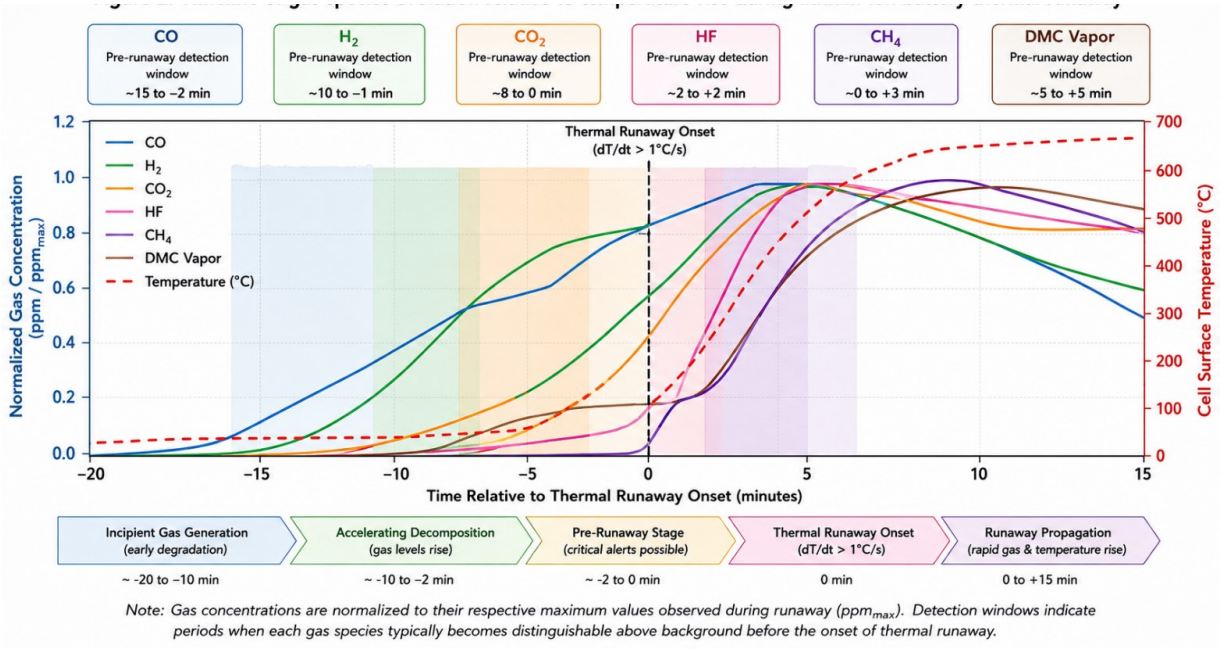


Figure 2. Timeline of gas species evolution relative to temperature increase during lithium-ion battery thermal runaway.

3. Gas sensor technologies for battery monitoring

3.1. Metal oxide semiconductor sensors

Metal oxide semiconductor (MOS) sensors detect gases by measuring the resistance changes in metal oxide films. Common materials include SnO_2, ZnO, TiO_2, WO_3, and In_2O_3. The target gases are adsorbed onto the film surface, where they undergo catalytic oxidation. This alters the electron density at the grain boundaries of the oxide. Reducing gases donate electrons to n-type oxide surface. Oxidizing molecules withdraw electrons from the surrounding environment. Both processes shift the electrical resistance of the sensor [32,33,35,40]. MOS sensors offer several practical advantages. They can detect CO, H_2, and VOCs at sub-ppm levels. They are low-cost, compact, and compatible with standard microelectronic fabrication processes. These properties make them widely used in gas-sensing applications [41-42]. However, their direct deployment in BMS environments remains challenging. MOS sensors respond to multiple gas species, thereby limiting their selectivity. Humidity interference is a persistent problem. Operating temperatures of 200–400°C require active thermal management inside the battery pack [34,45-46,48]. Recent advances in materials have addressed some limitations. Electrospun fiber architectures, core-shell heterostructures, and noble metal surface functionalization have been utilized. Pd, Pt, and Au dopants improve selectivity and enable room-temperature operation [43,49,71–74]. Doped SnO_2 sensors have achieved ppb-level sensitivities to CO and H_2. They also exhibited better discrimination against interfering gases such as ethanol vapor.

The integration of MEMS platforms further reduces power consumption. Some nanostructured MOS-MEMS devices currently operate at the milliwatt level. This power draw makes continuous onboard monitoring practical [36, 50-51]. MOS sensors remain dominant because of their low cost, compact size, high sensitivity, ease of integration with MEMS fabrication processes, robustness, and commercial availability. Although selectivity remains a challenge, recent advances in catalyst doping, nanostructuring, and sensor-array approaches significantly improve discrimination performance.

3.2. Electrochemical sensors

Amperometric electrochemical sensors measure the current produced by the working electrode. The target gas undergoes oxidation or reduction through a thin electrolyte layer. The current output was proportional to the gas concentration, providing a quantitative linear response. This response was observed across a wide concentration range. The electrode potential determines which gas species react, thereby providing inherent selectivity. The sensors operate at ambient temperatures, thereby removing the thermal management burden of MOS sensors [15]. These properties make them the standard materials for CO and H_2 detection in industrial environments. The deployment of BMSs poses several challenges. Electrolyte drying limits the sensor lifetime during long service periods. Pressure differentials inside hermetically sealed battery packs affect the readings of the sensors. HF present in thermal runaway gas mixtures corrodes the sensor components [14,15]. Solid polymer electrolyte variants can address this drying problem. They achieve service lifetimes of 3–5 years. Residential and industrial CO detectors have been commercially used. The research prototypes were tested under simulated battery-pack conditions. Modified PTFE membrane housings allow stable operation at temperatures of up to 60°C [14,15].

3.3. Optical and photoacoustic sensors

Non-dispersive infrared (NDIR) sensors detect gases by measuring infrared radiation absorption. Each gas absorbs IR radiation at characteristic wavelengths that are associated with its molecular vibrational modes. This gives NDIR sensors their inherent selectivity, as each target gas has a unique IR fingerprint. They do not require consumable electrolytes and resist the measurement drift over time. The sensitivity reaches ppm to sub-ppm levels for CO, CO_2, CH_4, and C_2H_4 [39]. Historically, NDIR sensors have been large and expensive for BMS integration. Their optical path requirements increase packaging complexity. Miniaturization is closing this gap. MEMS-fabricated absorption cells and VCSEL light sources have substantially reduced both their size and cost. Photoacoustic spectroscopy (PAS) operates based on different physical principles. The modulated laser radiation was absorbed by the target gas. This generated acoustic pressure waves that were measured using the sensor. PAS achieves ppb to sub-ppb sensitivity. Laboratory systems successfully detected HF and VOCs in the battery samples. However, PAS has not yet reached the cost and robustness required for automotive applications. Tunable diode laser absorption spectroscopy (TDLAS) is between NDIR and PAS in terms of its practical maturity. It has demonstrated sub-ppm sensitivity to H_2S and HF in industrial applications [39]. Automotive deployment is still in development.

3.4. Nanomaterial-based and emerging sensors

Carbon nanotubes (CNTs) and graphene exploit the high surface area-to-volume ratio of sp2 carbon atoms. Gas molecules adsorbed onto CNT or graphene surfaces produce measurable resistance changes in the sensor. This occurs at room temperature and does not require heating [37,38]. Therefore, the power consumption is lower than that of MOS sensors. The functionalization of these materials with metal nanoparticles or polymeric groups improves their selectivity for specific analytes. The target analytes were H_2, CO, and NO_2. CNT arrays analyzed using principal component analysis (PCA) can simultaneously discriminate between multiple gas species [44]. Metal-organic framework (MOF) materials offer tunable porosity for selective gas detection. Their host-guest chemistry pre-concentrates low-molecular-weight gases before measurement. MOF-coated quartz crystal microbalance (QCM) transducers were used to detect DMC vapor and CO_2 at concentrations below 10 ppm. Surface acoustic wave (SAW) transducers with MOF coatings show similar performance with high discrimination between species [31]. MXenes, particularly $Ti_3C_2T_x$, have recently emerged as sensing platforms at room temperature. They combine high electrical conductivity with chemically active surface groups to achieve high performance. The demonstrated targets included NH_3, CO_2, and H_2 at ppb levels. The large-scale deployment of automotive packs remains in the research stage.

Polymer-based optical fibers with chemically sensitive cladding represent an emerging technology. Unlike point sensors, these sensors can detect gases along their entire length. This enables distributed sensing throughout the entire battery pack. Large-format automotive and stationary storage packs benefit the most from this method. A single-point sensor may miss localized fault development in these configurations [25].

Table 2. Comparative performance summary of gas sensor technologies for EV battery management applications

Sensor Type	**Target Gases**	**Sensitivity**	**Selectivity**	**Operating Temp.**	**Lifetime**	**BMS Suitability**	**Reference**
MOS (nanostructured)	CO, H_2, VOC, CH_4	Sub-ppm to ppm	Moderate (array improves)	150–400°C heater	3–5 years	High (MEMS variants)	[14]
Electrochemical (amperometric)	CO, H_2, HF, O_2	ppm to sub-ppm	High	Ambient	2–5 years	High	[15]
NDIR optical	CO, CO_2, CH_4, C_2H_4	ppm	Very high	Ambient	>10 years	Moderate (size/cost)	[33,37]
PAS / TDLAS	HF, VOCs, CO	ppb to sub-ppm	Very high	Ambient	>10 years	Low–Moderate (cost)	[34]
CNT / graphene	CO, H_2, NO_2, NH3	ppb	Moderate–High	Room temp.	Under study	Emerging	[35,36]
MOF-based (QCM/SAW)	DMC, CO_2, VOC	Sub-ppm to ppb	High (tunable)	Room temp.	Under study	Emerging	[36,37]
MXene (2D material)	NH3, CO_2, H_2	ppb	Moderate	Room temp.	Under study	Early stage	[37]
Optical fiber (distributed)	Multiple (cladding -dep.)	ppm	Moderate	Ambient	>5 years	High potential	[44,45]

The suitability of BMS reflects its packaging, cost, and environmental robustness for automotive deployment.

Based on Figure 3, MOF and electrochemical sensors are identified as the most mature technologies currently suitable for commercial EV battery packs, while optical, photoacoustic, MOF-based, MXene-based, and advanced nanomaterial sensors are discussed as emerging technologies that remain largely at the laboratory or prototype stage.

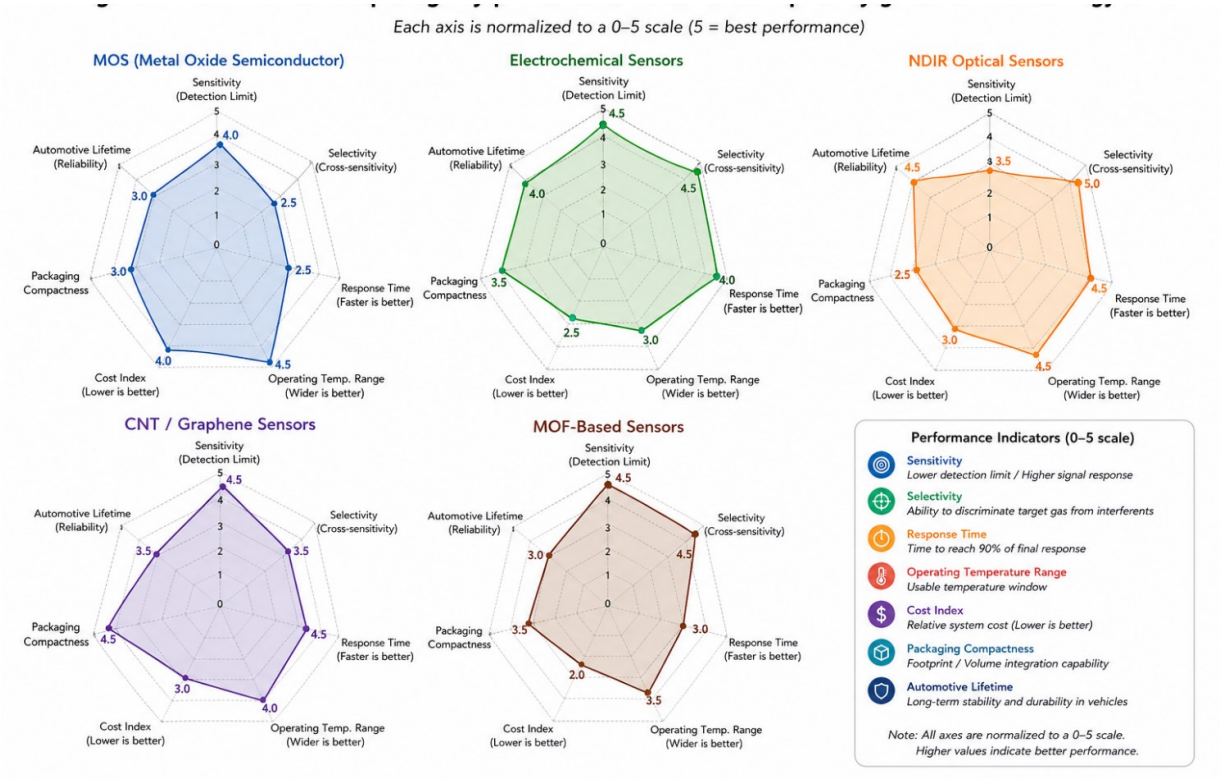


Figure 3. Radar charts comparing key performance indicators (sensitivity, selectivity, response time, operating temperature range, cost index, packaging compactness, and automotive lifetime) of the five primary sensor technology classes.

4. IoT architectures for intelligent battery gas monitoring

4.1. System architecture and layered framework

The IoT-integrated BMS gas monitoring architecture is divided into four functional layers. The first is the physical sensing layer. It contains gas sensors, temperature probes, voltage monitors, and current monitors. Environmental sensors are also included in the battery-pack enclosure. The second layer is the edge computing layer. Microcontrollers (MCUs) or system-on-chip (SoC) processors are co-located with battery packs. They handle real-time signal conditioning and feature extraction. On-device AI inference also runs in this layer as well. The third is the connectivity layer. The processed sensor data are transferred to vehicle telematics units and fleet management servers. OEM cloud platforms also receive data from this layer. Communication is implemented using secure wireless and wired protocols. The fourth layer is the analytics and response layer. Cloud-hosted ML models run fleet-level anomaly detections. This layer also handles predictive maintenance scheduling, regulatory reporting, and firmware updates [52,53]. This architecture follows the established IoT edge-cloud continuum model. It is specifically adapted to the safety requirements of automotive batteries. Three constraints drive this adaptation: latency, reliability, and the functional safety of the system. Critical safety decisions must be made at the edge. An example of this is the triggering of the battery isolation

contactors. The initiation of a thermal management response is another important factor. Both must occur within tens of milliseconds of fault detection. However, the cloud round-trip latency is too slow for these decisions [54].

Noncritical tasks are suitable for cloud-based offloading. Health trend estimation falls into this category. Fleet-level degradation correlations are also applicable. Separating time-critical and non-critical tasks in this manner ensures a rapid safety response.

4.2. IoT hardware platforms for on-vehicle gas monitoring

Several commercial IoT platforms are suitable for developing BMS gas-monitoring prototypes. The ESP32, STM32, and Nordic nRF52 series are widely used in IoT applications. All three offer integrated analog-to-digital conversion and I2C/SPI sensor interfaces. Wi-Fi and Bluetooth LE connectivity are built in. Cryptographic accelerators are included within sub-100 mW power envelopes. Production deployment requires automotive-grade hardware. Prototype platforms do not meet automotive functional safety standards. The Renesas RH850 and NXP S32K series microcontrollers were certified to ISO 26262. They provide hardware fault tolerance and ASIL-B/D compliance. Safety-critical vehicle functions require this level of certification [64]. MEMS sensor dies can be directly integrated onto BMS circuit boards. Alternatively, they can be housed in modular nodes attached to the pack ventilation path. The placement within the pack significantly affected response time. The sensors near the electrolyte vent ports responded the fastest to cell-level outgassing. They are closest to the gas source at the individual cell group level. Sensors in the pack headspace detect module-level gas accumulation earlier. Each placement strategy captures a different stage of fault progression [9,11]. Effective monitoring systems utilize both types of data.

4.3. Machine Learning Approaches for Gas Data Analysis

A simple threshold comparison is insufficient for multi-gas and multi-sensor data streams. IoT BMS monitoring systems generate complex overlapping signals from several sources. Therefore, more sophisticated analytical methods are required. Several machine learning approaches have been applied in this area. Classical supervised methods include support vector machines, random forests, and gradient boosting. Unsupervised anomaly detection uses autoencoders and the isolation forest algorithm. Deep learning options include long short-term memory (LSTM) networks and transformer-based architectures [55,56,57]. CNNs have been applied to the time-frequency representations of multi-gas sensor array signals. Laboratory studies have reported 97–99% accuracy in distinguishing battery fault events from background noise. LSTM networks were trained on sequences of CO, H_2, CO_2, and temperatures. The training data were obtained from controlled thermal runaway induction experiments conducted in this study. These models predicted the thermal runaway onset 6–12 min in advance. They achieved high sensitivity with low false-alarm rates [58]. The XGBoost models also exhibited strong performance in thermal state estimation. They were applied to the normalized heat release rate data from the battery packs. The gas proxy variables were used as model inputs. The predictive accuracy reached $R^2 > 0.94$ [26,44]. Labeled fault data from actual vehicles are scarce. Transfer learning directly addresses this limitation. Models pretrained on synthetic or laboratory datasets are fine-tuned on small-field datasets. This approach is applicable to different battery chemistries and packaging configurations. Federated learning offers additional practical advantages. The models are trained and distributed across the vehicle fleets. The raw sensor data never leave the individual vehicles. Fleet-scale model improvement occurs without centralizing the sensitive data. This approach satisfies data sovereignty requirements across different regulatory jurisdictions. Multi-sensor fusion combining gas, temperature, voltage, current, and pressure measurements significantly improves the accuracy of early battery fault detection and reduces false alarms. Real-time fault classification in EV battery packs requires low-latency machine-learning models capable of operating within the computational constraints of automotive embedded hardware. Lightweight algorithms such as Random Forests, XGBoost, SVMs, and compact CNNs are generally more suitable for onboard

BMS deployment than computationally intensive deep-learning architectures. Model compression techniques, including pruning, quantization, and knowledge distillation, enable efficient edge-AI implementation while maintaining acceptable diagnostic performance. Future EV battery monitoring systems should prioritize robust sensor fusion, low-latency edge inference, and safety-compliant real-time decision making to ensure reliable thermal-runaway early warning.

4.4. Communication Protocols and Cybersecurity

In-vehicle communication between the BMS nodes and vehicle ECU uses standard automotive protocols. The primary options are the CAN bus (ISO 11898), CAN-FD, and Automotive Ethernet (100BASE-T1). Protocol selection depends on the data bandwidth requirements. The gas sensor sampling rates typically range from 1–10 Hz. CAN-FD handles this data rate easily.

Vehicles with external connectivity require additional communication interfaces. Cellular links using 4G LTE or 5G connect the BMS telematics unit to OEM cloud platforms. Wi-Fi provides an alternative when cellular coverage is not available. Both interfaces use TLS 1.3-encrypted channels for data transmission [54]. Cybersecurity is an underappreciated aspect of IoT BMS design and implementation. A compromised BMS can mask genuine fault conditions. Spoofed sensor data can suppress alerts during thermal events. Both scenarios pose direct safety risks to the vehicle occupants.

Two standards govern the cybersecurity requirements for connected vehicle systems: ISO/SAE 21434 mandates threat and risk assessments throughout the vehicle development life cycle. The UNECE WP.29 Regulation 155 requires secure boot and intrusion detection capabilities [64]. IoT BMS implementations must satisfy both of these requirements. Four security measures are required. The hardware root of trust prevents unauthorized firmware modification. Authenticated sensor data streams block the spoofed readings from the source. Network-layer anomaly detection identifies unusual communication patterns. Together, these defend against both remote attacks and physical tampering.

IoT-enabled battery monitoring systems are vulnerable to cybersecurity threats such as sensor spoofing, false-data injection, firmware tampering, and communication-bus attacks. These attacks can manipulate gas sensor readings, disrupt fault diagnosis, and compromise battery safety decisions. Unauthorized OTA updates and malicious firmware modifications may disable critical safety functions or alter detection thresholds. Security measures including secure boot, encryption, authentication protocols, and hardware-rooted trust mechanisms are essential to protect system integrity. Additionally, anomaly-detection algorithms can identify suspicious sensor behavior and communication patterns, improving the resilience of connected battery management systems.

Table 3. Summary of AI/ML methods applied to gas-based BMS fault detection and prediction

ML Method	Input Data	Output	Reported Performance	Reference
XGBoost regression	Multi-gas array + temp.	NHR / SoH prediction	R^2 = 0.94–0.97	[44,26]
LSTM (deep RNN)	Temporal CO, H_2, CO_2, T	Thermal runaway onset time	6–12 min advance warning	[56,58]
CNN on spectrograms	Multi-gas time-frequency	Fault classification (6 classes)	97–99% accuracy	[55,44]
Autoencoder (unsupervised)	Normal operation baseline	Anomaly score / fault flag	AUC > 0.95 (lab)	[55]
Random Forest	Gas + V, I, T features	SoH classification	91% accuracy	[58,59]

		(5 bands)		
SVM with RBF kernel	MOS array (6 sensors)	Gas type discrimination	94% (6-gas panel)	[44]
Transformer (attention)	Multi-modal BMS signals	Multi-fault prognosis	Emerging; <95% reported	[57]
Federated learning	Distributed fleet data	Fleet-level model update	Active research area	[52,53]

Data compiled from the referenced literature. NHR, normalized heat release rate; AUC, area under the ROC curve.

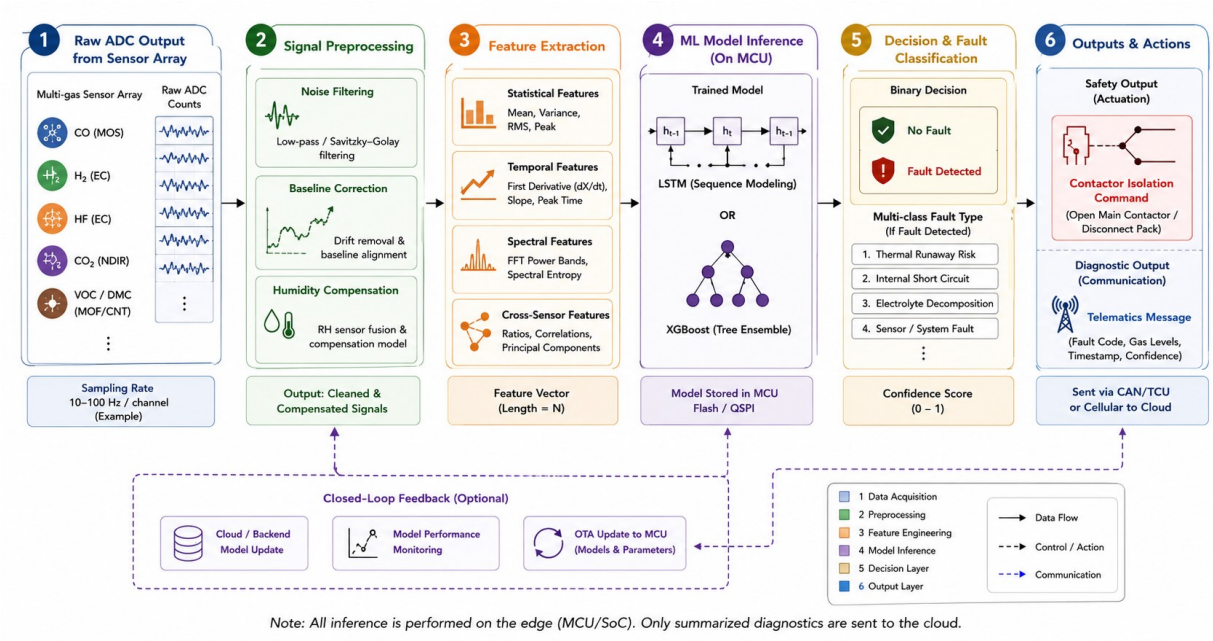


Figure 4. Block diagram of the ML inference pipeline for on-edge gas-fault detection.

5. Challenges

5.1. Cross-sensitivity and sensor selectivity

The electrochemical environment inside a battery pack is chemically complex. It also changes over time as cells age and cycle through the cell cycle. Humidity, ambient CO_2, electrolyte vapor, and polymer off-gassing are always present in the environment of the cell. These background species interfere with the detection of the target gases. Sensors must reliably discriminate between target gases and this interferent matrix. MOS sensors face significant challenges in terms of selectivity. Their response profiles are broad and overlap with those of multiple gas species. Therefore, single-sensor interpretation is unreliable in such environments. Multisensor arrays combined with pattern recognition algorithms can reduce this problem. However, arrays increase system complexity, power consumption, and calibration burden [14,33,34]. HF detection presents a different set of challenges. HF is highly reactive and does not travel far from its source. It is consumed on packaging surfaces before reaching the sensor. It also degrades the sensing elements via corrosive attacks. All components

of the gas sampling path were affected. Adhesives, seals, and PCB conformal coatings must be compatible with HF. Therefore, material selection across the entire sampling path is nontrivial. However, testing under realistic battery-pack conditions remains limited. Few published studies have exposed sensors to combined humidity, electrolyte vapor, and HF simultaneously. Background interferent mixtures in real packs are rarely replicated in laboratory evaluations. This gap leaves the sensor performance under true operating conditions poorly characterized [14,33,34].

5.2. Packaging, thermal management, and environmental constraints

The physical environment inside an automotive battery pack is hostile to sensitive sensors, such as temperature sensors. The operating temperatures range from −40°C to +85°C for automotive applications. Vibration and mechanical shock loads are continuous during vehicle operation. Moisture and electrolyte vapor enter the enclosure over time. Electromagnetic interference from power electronics adds stress. The sensor packaging must maintain a calibration stability across the entire temperature range. Condensation at low temperatures can trigger false gas readings. Packaging solutions must prevent this without blocking gas access to the sensing element. Most commercial MOS and electrochemical sensors have consumer or industrial temperature ratings. These ratings fall short of automotive AEC-Q100/Q101, ISO 16750 and USCAR-2 requirements. Therefore, a significant gap exists between laboratory demonstrations and production deployments [64]. Thermal management systems inside battery packs also affect gas transport. Liquid cooling circuits and phase-change materials alter airflow patterns within enclosures. The transition from conventional module-based battery packs to Cell-to-Pack (CTP) architectures introduces additional challenges for gas-sensor deployment. The removal of intermediate modules reduces enclosure headspace and alters gas-flow pathways, causing vent gases released from a failing cell to disperse differently throughout the pack. Furthermore, liquid-cooling systems generate localized airflow patterns and temperature gradients that can accelerate, redirect, or dilute gas transport before it reaches the sensor. Consequently, sensor response latency becomes highly dependent on pack geometry, cooling-channel configuration, vent locations, and sensor placement. A sensor positioned near a natural airflow pathway may detect fault gases significantly earlier than one located in a stagnant region of the enclosure. Therefore, Computational Fluid Dynamics (CFD)-based optimization is increasingly recognized as an essential design tool for predicting gas dispersion behavior, minimizing detection delays, and determining optimal sensor locations in modern CTP battery systems, thereby improving the effectiveness of thermal-runaway early-warning strategies.

5.3. Data latency, edge AI limitations, and model reliability

Deep learning models for gas fault detection require large labeled training datasets. These datasets must cover the entire range of fault conditions in the system. All battery chemistry variations, pack configurations, and environmental states should be represented. However, assembling such datasets is practically difficult. Controlled thermal runaway experiments are costly. They can also be potentially destructive to the test hardware. Field-collected fault data from actual vehicles are scarce. However, the available data are unevenly distributed across fault severity levels. Models trained on incomplete datasets generalize poorly to previously unobserved conditions. False alarm rates in production deployments can become unacceptable [55,57]. Edge inference faces separate hardware limitations. Automotive microcontrollers have limited computational resources and memory capacities. A typical production MCU may have only 512 KB of RAM. Large transformer models with billions of parameters cannot be executed on such hardware. Therefore, model compression techniques are required. Quantization reduces the numerical precision of model weights. Pruning removes low-contribution connections from the trained network. Knowledge distillation involves training a smaller model to replicate the larger model. All three techniques reduced the model size and inference times. The target was a sub-10 ms inference latency on the automotive hardware. The classification accuracy must be maintained during the compression process.

5.4. Regulatory gaps and standardization

Although several international standards address the safety of EV battery systems, the integration of gas sensing into Battery Management Systems (BMS) remains only partially covered. Standards such as ISO 6469-1, IEC 62133, and UNECE Regulation No. 100 (R100) primarily focus on electrical safety, thermal management, insulation integrity, and protection against short circuits and thermal events [61–63]. However, unlike earlier assumptions, battery-gas monitoring is no longer entirely absent from regulatory frameworks. Most notably, China's GB 38031-2020, mandatory since January 2021, requires electric vehicles to provide a thermal-runaway warning at least five minutes before a hazardous event, making it one of the most influential regulatory drivers for the adoption of gas-sensing and early-warning technologies in EV battery packs [64,65].

Despite this progress, significant gaps remain regarding the standardization of gas-sensor performance, sensor placement, calibration procedures, response-time requirements, and functional-safety classification [62,63,66]. Regulatory approaches also vary across regions. China has established clear thermal-runaway warning requirements through GB 38031-2020, while the European Union continues to rely primarily on UNECE R100 and related vehicle safety regulations [64,67]. In the United States, EV battery safety is governed through a combination of UL standards, SAE guidelines, and FMVSS requirements, but no dedicated gas-monitoring standard currently exists [68]. Similarly, the Indian regulatory framework, including ARAI and BIS approval processes, does not yet contain specific requirements for onboard battery gas sensing despite the rapid growth of EV adoption under FAME-II and PM e-DRIVE initiatives [69,70].

The absence of globally harmonized requirements creates challenges for OEMs in defining sensor performance targets, validating system reliability, and demonstrating compliance across different markets [66,68]. Future regulatory development should focus on harmonizing Chinese, European, US, and Indian frameworks while establishing standardized requirements for gas-sensor integration, testing protocols, functional safety, and thermal-runaway early-warning performance [64–70]. Such harmonization would accelerate commercialization and improve the safety consistency of next-generation EV battery systems worldwide.

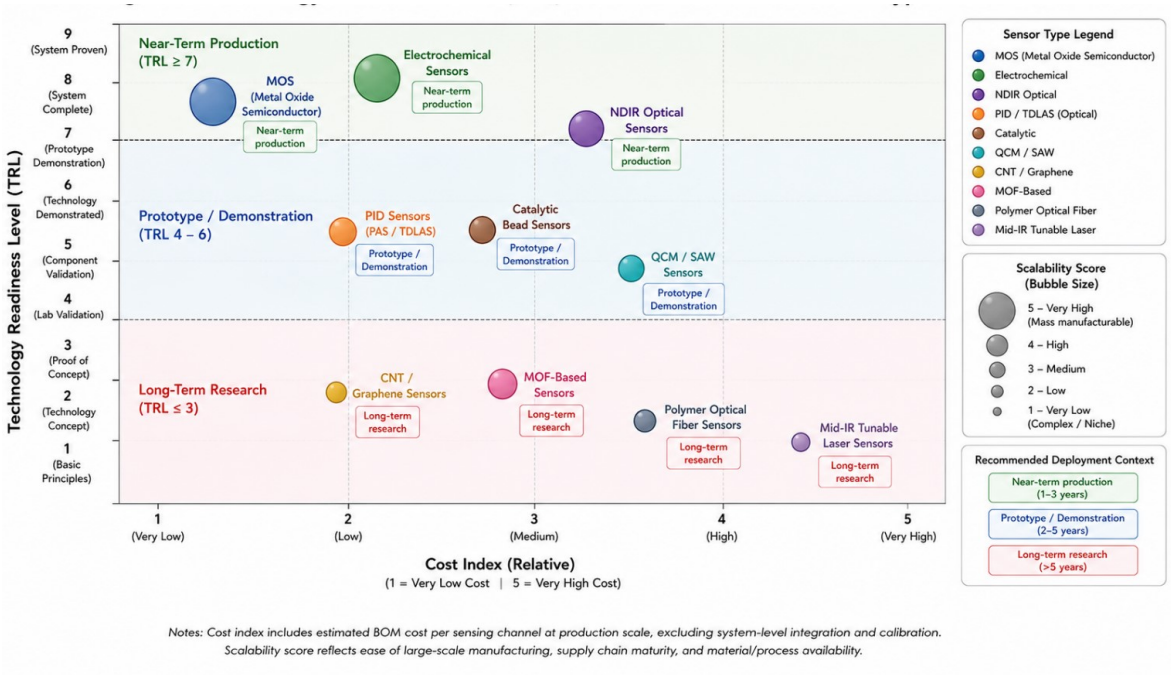


Figure 5. Technology readiness level (TRL) vs. cost index chart for all sensor types reviewed, plotted as a scatter diagram.

6. Future research directions

6.1. Multi-gas sensor fusion and holistic BMS integration

Future BMS architectures will integrate multiple sensor modalities into a single framework to achieve optimal performance. Gas, acoustic emission, strain, temperature, and impedance spectroscopy data arecombined. Each modality captures a different physical aspect of cell condition. No single modality can reliably detect all fault types. Bayesian sensor fusion approaches can combine the evidence from these physical observables. Ensemble ML models offer an alternative approach to achieve this goal. Both approaches improve the fault detection specificity compared to single-sensor systems. False alarm rates decrease when multiple independent signals must be agreed upon [58,60]. Standardized data interfaces are required to support this integration process. Current battery management system (BMS) communication protocols do not accommodate gas-sensor data fields. ISO 15118 governs battery state communication between vehicles and infrastructure. The extensions of ISO 15118 should include gas sensor data as defined fields. This would enable interoperability across vehicle platforms, original equipment manufacturers (OEMs), and service ecosystems.

6.2. Large language model and generative AI-assisted diagnostics

Large language models (LLMs) offer new capabilities for the interpretation of BMS faults. Standard ML models output labels or probability scores. LLMs can generate diagnostic reports in natural language. These reports can directly guide field technicians through inspection and remediation steps.

Fine-tuning the relevant data sources could improve the diagnostic accuracy. Battery failure mode databases, gas chemistry literature, and historical fault records are suitable sources of information for this purpose. A fine-tuned LLM can simultaneously synthesize evidence from multiple gas channels. This could then produce chemistry-specific fault interpretations in a plain language.

Retrieval-augmented generation (RAG) further enhances this capability. RAG systems retrieve relevant technical documentation for inference. They do not rely solely on knowledge encoded during training. This is important because the cell chemistries and pack configurations vary widely across the EV fleet. A RAG-based system can adapt its interpretation to the specific chemistry being studied. Static fine-tuned models cannot perform this task flexibly.

6.3. Digital twin integration for predictive maintenance

Digital twin models can couple multiple physical domains into a single simulation model. The three components are electrochemical degradation models, gas generation kinetics, and pack-level computational fluid dynamics (CFD) transport simulations. The combination of these data allows the gas sensor data to drive quantitative predictions. The remaining useful life (RUL) and thermal runaway risk probability are selected as the target outputs. Static models are insufficient for this purpose. The battery condition changes continuously during operation. The digital twin must remain synchronized with the live sensor telemetry. Kalman and particle filters provide state estimation mechanisms for this purpose. Both approaches update the internal state of the twin as new sensor data are received. The result is a probabilistic health monitoring framework. This is more informative than fixed-threshold alarms [25,54]. This research lies at the intersection of three fields. Electrochemical modeling provides degradation physics information. Computational fluid dynamics (CFD) handles gas transport within the pack geometry. Machine learning manages state estimation and pattern recognition in the sensor streams. No single research group currently covers all three topics with equal depth or comprehensively. This gap represents an open frontier for future research.

6.4. Solid-state battery-compatible sensing

Solid-state batteries (SSBs) replace liquid electrolytes with inorganic sulfides, oxides, or polymer alternatives. This change fundamentally alters the gas-generation signature of battery failure. Sensor technologies developed for liquid electrolyte cells cannot be directly applied to solid-state batteries. Sulfide-based solid electrolytes produce H_2S when exposed to moisture. This differs from the CO, HF, and hydrocarbon signatures of conventional lithium-ion batteries. Dendrite growth in SSBs generates localized resistive heating. This heating may be detectable through acoustic emissions rather than gas efflux. Some SSB failure modes may not produce gas signals. Current gas-sensing research has not systematically addressed the failure chemistry of SSBs. The concentration ranges, temperature profiles, and gas species relevant to SSB faults are poorly characterized [66]. Sensor materials and packaging suitable for H_2S detection in solid-electrolyte environments remain undeveloped. This is a concrete gap that must be filled before SSBs are mass deployed.

6.5. Self-calibrating and self-healing sensor systems

Automotive gas sensors must maintain their accuracy over long deployment periods. Physical recalibration in the field is rarely practical. Therefore, sensors must detect and compensate for drift and contamination. Dual-sensor differential architectures directly address baseline drift. One sensor remains active and is exposed to the packaging atmosphere. The second sensor is sealed in a reference gas environment. The difference between their outputs isolates the drift from genuine gas signals. AI-driven self-calibration offers a complementary approach. Models trained on the baseline gas chemistry of healthy batteries serve as dynamic references. The battery itself effectively serves as a calibration standard. This extends the sensor accuracy without requiring a physical intervention [26,53]. Two further research directions are required to determine the viability of production. Self-healing sensing materials are in the first category. MOFs with regenerable binding sites can recover their sensitivity after exposure to contaminants. The second is built-in self-test (BIST) architecture. BIST circuits verify the functionality of the sensor nodes during normal operation. Both are required before long-lifetime automotive deployments become reliable.

7. Conclusion

This review examined IoT-integrated gas sensing as an emerging technology for EV battery management. The principal conclusions are as follows.

- Gas generation is an intrinsic feature of lithium-ion battery degradation. CO, H_2, HF, CH_4, and VOCs appeared 6–15 min before the temperature increase was detectable. This chemical warning window precedes any electrical or thermal signals that can be measured by a conventional BMS.
- No single sensor technology meets all the requirements for the deployment of BMS. MOS, electrochemical, optical, and nanomaterial-based platforms offer different performance profiles. Multimodal sensor arrays combined with ML-based pattern recognition provide the best balance of these factors. The sensitivity, selectivity, and false-alarm robustness were improved using this approach.
- IoT architectures enable capabilities that are unavailable in conventional threshold-based BMS designs. Edge AI inference supports real-time safety responses in milliseconds. Cloud analytics supports long-term predictive maintenance across vehicle fleets. Secure connectivity links both layers without introducing unacceptable latency.
- Several challenges must be addressed before large-scale production can be deployed. The automotive qualification of gas sensors is incomplete. Calibration stability under harsh pack environments has not been proven for the entire vehicle lifetime. Labeled training data for fault

classification are limited. Regulatory standards for BMS gas monitoring are currently unavailable. Cybersecurity frameworks for connected sensor nodes are still under development.

- Five research directions offer the highest near-term returns. Multimodal sensor fusion improves fault discrimination without adding sensors to the system. LLM-assisted diagnostics translate sensor data into actionable technician guidance. Digital twin integration converts gas readings into quantitative RUL predictions. Solid-state battery-compatible sensing addresses a gap that will widen as SSBs enter the market. Self-calibrating sensor architectures extend the deployment lifetime without physical intervention.
- The global EV fleet is expected to exceed 300 million vehicles within the next decade. At this scale, gas-aware BMS technology is no longer optional and is essential. This has become a safety requirement in the industry. This review maps the existing capabilities, challenges, and promising research directions. The goal is to provide researchers and engineers with a clear starting point.

Sensor reliability remains the most significant challenge for the commercialization of gas-sensing-based battery management systems, as sensors must operate accurately under harsh battery-pack conditions including high temperatures, humidity, vibration, and exposure to corrosive gases. Long-term sensor drift, material degradation, and cross-sensitivity can compromise the accuracy of early fault detection and reduce system reliability. Therefore, developing durable, selective, and self-calibrating sensors capable of maintaining stable performance throughout the vehicle lifetime is essential for widespread industrial adoption.

Acknowledgements

The authors acknowledge the research support of DDU Kaushal Kendra, Dr. Babasaheb Ambedkar Marathwada University, Chhatrapati Sambhajinagar, India.

Conflict of Interest

The authors declare that they have no known competing financial interests or personal relationships that could influence the work reported in this study.

References

[1] Arora, P., & Zhang, Z. (. (2004). Battery separators. *Chemical Reviews*, 104(10), 4419–4462. https://doi.org/10.1021/cr020738u

[2] Feng, X., Ouyang, M., Liu, X., Lu, L., Xia, Y., & He, X. (2018). Thermal runaway mechanism of lithium-ion batteries for electric vehicles: A review. *Energy Storage Materials*, 10, 246–267. https://doi.org/10.1016/j.ensm.2017.05.013.

[3] Lisbona, D., & Snee, T. (2011). A review of the hazards associated with primary lithium and lithium-ion batteries. *Process Safety and Environmental Protection*, 89(6), 434–442. https://doi.org/10.1016/j.psep.2011.06.022.

[4] Koch, S., Fill, A., & Birke, K. P. (2018). Comprehensive gas analysis of large-scale automotive lithium-ion cells during thermal runaway. *Journal of Power Sources*, 398, 106–112. https://doi.org/10.1016/j.jpowsour.2018.07.051.

[5] Golubkov, A. W., Fuchs, D., Wagner, J., Wiltsche, H., Stangl, C., Fauler, G., Voitic, G., Thaler, A., & Hacker, V. (2014). Thermal-runaway experiments on consumer Li-ion batteries with metal-oxide and olivine-type cathodes. *RSC Adv.*, 4(7), 3633–3642. https://doi.org/10.1039/c3ra45748f.

[6] Larsson, F.; Andersson, P.; Blomqvist, P.; Mellander, B.-E. (2017). Toxic fluoride gas emissions from lithium-ion battery fires. *Scientific Reports*, 7(1), 10018. https://doi.org/10.1038/s41598-017-09784-z.

[7] Sturk, D., Rosell, L., Blomqvist, P., & Ahlberg Tidblad, A. (2019). Analysis of Li-Ion battery gases vented in an inert atmosphere thermal test chamber. *Batteries*, 5(3), 61. https://doi.org/10.3390/batteries5030061.

[8] Essl, C., Golubkov, A. W., Gasser, E., Nachtnebel, M., Zankel, A., Ewert, E., & Fuchs, A. (2020). Comprehensive hazard analysis of failing automotive lithium-ion batteries in over-temperature experiments. *Batteries*, 6(2), 30. https://doi.org/10.3390/batteries6020030.

[9] Örs, E. F. & Javani, N. (2026). Early detection of thermal runaway in lithium-ion batteries under extreme conditions using phase change materials. *Thermal Science and Engineering Progress*, 70, 104502. https://doi.org/10.1016/j.tsep.2026.104502.

[10] Doughty, D., & . (2012). Vehicle battery safety roadmap guidance (Ed.). *Office of Scientific and Technical Information (OSTI)*. https://doi.org/10.2172/1055366.

[11] Cai, T., Stefanopoulou, A. G., & Siegel, J. B. (2019). Early detection for Li-Ion batteries thermal runaway based on gas sensing. *ECS Meeting Abstracts*, MA2019-01(6), 586. https://doi.org/10.1149/ma2019-01/6/586.

[12] Wang, Q., Ping, P., Zhao, X., Chu, G., Sun, J., & Chen, C. (2012). Thermal runaway caused fire and explosion of lithium ion battery. *Journal of Power Sources*, 208, 210–224. https://doi.org/10.1016/j.jpowsour.2012.02.038.

[13] Sun, P., Bisschop, R., Niu, H., & Huang, X. (2020). A review of battery fires in electric vehicles. *Fire Technology*, 56(4), 1361–1410. https://doi.org/10.1007/s10694-019-00944-3.

[14] Zhou, K., & Liu, Y. (2021). Early-stage gas identification using convolutional long short-term neural network with sensor array time series data. *Sensors*, 21(14), 4826. https://doi.org/10.3390/s21144826.

[15] Lohrberg, O., Maletti, S., Heubner, C., Schneider, M., & Michaelis, A. (2022). Understanding Li plating and stripping behavior in zero-excess Li metal batteries using operando dilatometry. *Journal of the Electrochemical Society*, 169(3), 30543. https://doi.org/10.1149/1945-7111/ac5cf1.

[16] Liu, X., Ren, D., Hsu, H., Feng, X., Xu, G.-L., Zhuang, M., Gao, H., Lu, L., Han, X., Chu, Z., Li, J., He, X., Amine, K., & Ouyang, M. (2018). Thermal runaway of lithium-ion batteries without internal short circuit. *Joule*, 2(10), 2047–2064. https://doi.org/10.1016/j.joule.2018.06.015.

[17] Zhang, Y., Wang, H., Li, W., & Li, C. (2019). Quantitative identification of emissions from abused prismatic Ni-rich lithium-ion batteries. *eTransportation*, 2, 100031. https://doi.org/10.1016/j.etran.2019.100031.

[18] Mikolajczak, C., Kahn, M., White, K., & Long, R. T. (2012). Lithium-ion fire hazard assessment. In *Lithium-Ion Batteries Hazard and Use Assessment* (pp. 85-104). Boston, MA: Springer US. https://doi.org/10.1007/978-1-4614-3486-3_6.

[19] Peled, E., & Menkin, S. (2017). Review—SEI: Past, present and future. *Journal of the Electrochemical Society*, 164(7), A1703–A1719. https://doi.org/10.1149/2.1441707jes.

[20] Spotnitz, R., & Franklin, J. (2003). Abuse behavior of high-power, lithium-ion cells. *Journal of Power Sources*, 113(1), 81–100. https://doi.org/10.1016/s0378-7753(02)00488-3.

[21] Islam, M. S., & Fisher, C. A. J. (2014). Lithium and sodium battery cathode materials: Computational insights into voltage, diffusion and nanostructural properties. *Chem. Soc. Rev.*, 43(1), 185–204. https://doi.org/10.1039/c3cs60199d.

[22] Ren, D., Feng, X., Lu, L., Ouyang, M., Zheng, S., Li, J., & He, X. (2017). An electrochemical-thermal coupled overcharge-to-thermal-runaway model for lithium ion battery. *Journal of Power Sources*, 364, 328–340. https://doi.org/10.1016/j.jpowsour.2017.08.035.

[23] Bernhard, R., Meini, S., & Gasteiger, H. A. (2014). On-line electrochemical mass spectrometry investigations on the gassing behavior of Li4Ti5O12 electrodes and its origins. *Journal of The Electrochemical Society*, 161(4), A497. https://doi.org/10.1149/2.013404jes

[24] Janek, J., & Zeier, W. G. (2016). A solid future for battery development. *Nature Energy*, 1(9). https://doi.org/10.1038/nenergy.2016.141.

[25] Duquennoy, M., Smagin, N., Kadi, T., Ouaftouh, M., & Jenot, F. (2022). Development of a broadband (100–240 MHz) surface acoustic wave emitter devoted to the non-destructive characterization of sub-micrometric thin films. *Sensors*, 22(19), 7464. https://doi.org/10.3390/s22197464.

[26] Abidin, A. Z., Enriko, I. K. A., & Pramudita, A. A. (2025). Leveraging IoT, digital twin and machine learning for smart energy audit in office building: A systematic literature review and recommendations. *E-Prime - Advances in Electrical Engineering, Electronics and Energy*, 14, 101124. https://doi.org/10.1016/j.prime.2025.101124.

[27] Wang, Z., Yang, H., Li, Y., Wang, G., & Wang, J. (2019). Thermal runaway and fire behaviors of large-scale lithium ion batteries with different heating methods. *Journal of Hazardous Materials*, 379, 120730. https://doi.org/10.1016/j.jhazmat.2019.06.007.

[28] Chen, M., Liu, J., He, Y., Yuen, R., & Wang, J. (2017). Study of the fire hazards of lithium-ion batteries at different pressures. *Applied Thermal Engineering*, 125, 1061–1074. https://doi.org/10.1016/j.applthermaleng.2017.06.131.

[29] Chombo, P. V., & Laoonual, Y. (2020). A review of safety strategies of a Li-ion battery. *Journal of Power Sources*, 478, 228649. https://doi.org/10.1016/j.jpowsour.2020.228649.

[30] Miao, Y., Hynan, P., von Jouanne, A., & Yokochi, A. (2019). Current Li-Ion battery technologies in electric vehicles and opportunities for advancements. *Energies*, 12(6), 1074. https://doi.org/10.3390/en12061074.

[31] Kumar, P., Kim, K.-H., Bansal, V., Paul, A. K., & Deep, A. (2016). Practical utilization of nanocrystal metal organic framework biosensor for parathion specific recognition. *Microchemical Journal*, 128, 102–107. https://doi.org/10.1016/j.microc.2016.04.008.

[32] Yoon, J.-W., & Lee, J.-H. (2017). Toward breath analysis on a chip for disease diagnosis using semiconductor-based chemiresistors: recent progress and future perspectives. *Lab Chip*, 17(21), 3537–3557. https://doi.org/10.1039/c7lc00810d.

[33] Kim, H.-J., & Lee, J.-H. (2014). Highly sensitive and selective gas sensors using p-type oxide semiconductors: Overview. *Sensors and Actuators B: Chemical*, 192, 607–627. https://doi.org/10.1016/j.snb.2013.11.005.

[34] Mirzaei, A., Leonardi, S. G., & Neri, G. (2016). Detection of hazardous volatile organic compounds (VOCs) by metal oxide nanostructures-based gas sensors: A review. *Ceramics International*, 42(14), 15119–15141. https://doi.org/10.1016/j.ceramint.2016.06.145.

[35] Dey, A. (2018). Semiconductor metal oxide gas sensors: A review. *Materials Science and Engineering: B*, 229, 206–217. https://doi.org/10.1016/j.mseb.2017.12.036.

[36] Sheng, G., & Xu, J. (2014). Nanoscale dynamics of MEMS TFC active slider. *Microsystem Technologies*, 20(8-9), 1767–1770. https://doi.org/10.1007/s00542-014-2244-2.

[37] Llobet, E. (2013). Gas sensors using carbon nanomaterials: A review. *Sensors and Actuators B: Chemical*, 179, 32–45. https://doi.org/10.1016/j.snb.2012.11.014.

[38] Lee, C., Wei, X., Kysar, J. W., & Hone, J. (2008). Measurement of the elastic properties and intrinsic strength of monolayer graphene. *Science*, 321(5887), 385–388. https://doi.org/10.1126/science.1157996.

[39] Zhou, X., Lee, S., Xu, Z., & Yoon, J. (2015). Recent progress on the development of chemosensors for gases. *Chemical Reviews*, 115(15), 7944–8000. https://doi.org/10.1021/cr500567r.

[40] Knapp, C. E., Kafizas, A., Parkin, I. P., & Carmalt, C. J. (2011). The use of combinatorial aerosol-assisted chemical vapour deposition for the formation of gallium-indium-oxide thin films. *Journal of Materials Chemistry*, 21(34), 12644. https://doi.org/10.1039/c1jm11606a.

[41] Perera, A. G. U., Jayaweera, P. V. V., Ariyawansa, G., Matsik, S. G., Tennakone, K., Buchanan, M., Liu, H. C., Su, X. H., & Bhattacharya, P. (2009). Room temperature nano- and microstructure photon detectors. *Microelectronics Journal*, 40(3), 507–511. https://doi.org/10.1016/j.mejo.2008.06.019.

[42] Moon, H. G., Shim, Y.-S., Kim, D. H., Jeong, H. Y., Jeong, M., Jung, J. Y., Han, S. M., Kim, J. K., Kim, J.-S., Park, H.-H., Lee, J.-H., Tuller, H. L., Yoon, S.-J., & Jang, H. W. (2012). Self-activated ultrahigh chemosensitivity of oxide thin film nanostructures for transparent sensors. *Scientific Reports*, 2(1). https://doi.org/10.1038/srep00588.

[43] Park, S., Kim, S., Ko, H., & Lee, C. (2014). Light-enhanced gas sensing of ZnS-core/ZnO-shell nanowires at room temperature. *Journal of Electroceramics*, 33(1-2), 75–81. https://doi.org/10.1007/s10832-014-9923-3.

[44] Huang, W.-C., Wei, C.-D., Belkin, S., Hsieh, T.-H., & Cheng, J.-Y. (2022). Machine-learning assisted antibiotic detection and categorization using a bacterial sensor array. *Sensors and Actuators B: Chemical*, 355, 131257. https://doi.org/10.1016/j.snb.2021.131257.

[45] Zhang, J., Liu, X., Neri, G., & Pinna, N. (2015). Nanostructured materials for room-temperature gas sensors. *Advanced Materials*, 28(5), 795–831. Portico. https://doi.org/10.1002/adma.201503825.

[46] Righettoni, M., Tricoli, A., & Pratsinis, S. E. (2010). Si:WO_3 sensors for highly selective detection of acetone for easy diagnosis of diabetes by breath analysis. *Analytical Chemistry*, 82(9), 3581–3587. https://doi.org/10.1021/ac902695n

[47] Waldmann, T., Wilka, M., Kasper, M., Fleischhammer, M., & Wohlfahrt-Mehrens, M. (2014). Temperature dependent ageing mechanisms in Lithium-ion batteries – A post-mortem study. *Journal of Power Sources*, 262, 129–135. https://doi.org/10.1016/j.jpowsour.2014.03.112.

[48] Wang, Y., & Cao, G. (2008). Developments in nanostructured cathode materials for high-performance lithium-ion batteries. *Advanced Materials*, 20(12), 2251–2269. Portico. https://doi.org/10.1002/adma.200702242.

[49] Kim, I. D., Rothschild, A., Lee, B. H., Kim, D. Y., Jo, S. M., & Tuller, H. L. (2006). Ultrasensitive chemiresistors based on electrospun TiO_2 nanofibers. *Nano Letters*, 6(9), 2009–2013. https://doi.org/10.1021/nl061197h

[50] Majewski, L. A., Balocco, C., King, R., Whitelegg, S., & Song, A. M. (2008). Fast polymer nanorectifiers for inductively coupled RFID tags. *Materials Science and Engineering*: B, 147(2-3), 289–292. https://doi.org/10.1016/j.mseb.2007.08.031.

[51] Manickam, S. S., & McCutcheon, J. R. (2015). Model thin film composite membranes for forward osmosis: Demonstrating the inaccuracy of existing structural parameter models. *Journal of Membrane Science*, 483, 70–74. https://doi.org/10.1016/j.memsci.2015.01.017.

[52] Soldatos, J. (2016). Building blocks for IoT analytics. *Building Blocks for IoT Analytics*, 1–294. https://doi.org/10.13052/rp-9788793519046.

[53] Ismail, S., Dawoud, D. W., Ismail, N., Marsh, R., & Alshami, A. S. (2022). IoT-based water management systems: Survey and future research direction. IEEE Access, 10, 35942–35952. https://doi.org/10.1109/access.2022.3163742.

[54] Ullah, Z., Wang, S., Wu, G., Xiao, M., Lai, J., & Elkadeem, M. R. (2022). Advanced energy management strategy for microgrid using real-time monitoring interface. *Journal of Energy Storage*, 52, 104814. https://doi.org/10.1016/j.est.2022.104814.

[55] LeCun, Y., Bengio, Y., & Hinton, G. (2015). Deep learning. *Nature*, 521(7553), 436–444. https://doi.org/10.1038/nature14539.

[56] Hochreiter, S., & Schmidhuber, J. (1997). Long Short-Term Memory. *Neural Computation*, 9(8), 1735–1780. https://doi.org/10.1162/neco.1997.9.8.1735.

[57] Yu, L., Zhang, H., & Xu, C. (2024). Text-guided attention is all you need for zero-shot robustness in vision-language models. *Advances in Neural Information Processing Systems,* 37, 96424–96448. https://doi.org/10.52202/079017-3056.

[58] Li, X., Wang, Z., Zhang, L., Zou, C., & Dorrell, David. D. (2019). State-of-health estimation for Li-ion batteries by combing the incremental capacity analysis method with grey relational analysis. *Journal of Power Sources*, 410-411, 106–114. https://doi.org/10.1016/j.jpowsour.2018.10.069.

[59] Yang, F., Wang, D., Zhao, Y., Tsui, K.-L., & Bae, S. J. (2018). A study of the relationship between coulombic efficiency and capacity degradation of commercial lithium-ion batteries. *Energy*, 145, 486–495. https://doi.org/10.1016/j.energy.2017.12.144.

[60] Jokar, A., Rajabloo, B., Désilets, M., & Lacroix, M. (2016). Review of simplified pseudo-two-dimensional models of lithium-ion batteries. *Journal of Power Sources*, 327, 44–55. https://doi.org/10.1016/j.jpowsour.2016.07.036.

[61] Electrically propelled road vehicles. Safety specifications. *BSI British Standards*. https://doi.org/10.3403/bsiso6469

[62] Secondary cells and batteries containing alkaline or other non-acid electrolytes. Experimental procedure for the forced internal short-circuit test of IEC 62133:2012. *BSI British Standards*. https://doi.org/10.3403/30298022.

[63] United Nations. (2020). Requirements concerning the construction and approval of vehicles. https://doi.org/10.18356/4cda7bd4-en.

[64] Safari, M. (2018). Battery electric vehicles: Looking behind to move forward. *Energy Policy*, 115, 54–65. https://doi.org/10.1016/j.enpol.2017.12.053.

[65] Xu, J., Cai, X., Cai, S., Shao, Y., Hu, C., Lu, S., & Ding, S. (2023). High-energy lithium-ion batteries: Recent progress and a promising future in applications. *Energy & Environmental Materials*, 6(5). Portico. https://doi.org/10.1002/eem2.12450.

[66] Liu, Q., Wang, L., & He, X. (2023). Toward practical solid-state polymer lithium batteries by in situ polymerization process: A review. *Advanced Energy Materials*, 13(30). Portico. https://doi.org/10.1002/aenm.202300798.

[67] Chen, Y., Kang, Y., Zhao, Y., Wang, L., Liu, J., Li, Y., Liang, Z., He, X., Li, X., Tavajohi, N., & Li, B. (2021). A review of lithium-ion battery safety concerns: The issues, strategies, and testing standards. *Journal of Energy Chemistry*, 59, 83–99. https://doi.org/10.1016/j.jechem.2020.10.017.

[68] Willenberg, L. K., Dechent, P., Fuchs, G., Sauer, D. U., & Figgemeier, E. (2020). High-precision monitoring of volume change of commercial lithium-ion batteries by using strain gauges. *Sustainability*, 12(2), 557. https://doi.org/10.3390/su12020557.

[69] Agubra, V., & Fergus, J. (2013). Lithium ion battery anode aging mechanisms. *Materials*, 6(4), 1310–1325. https://doi.org/10.3390/ma6041310.

[70] Tröltzsch, U., Kanoun, O., & Tränkler, H.-R. (2006). Characterizing aging effects of lithium ion batteries by impedance spectroscopy. *Electrochimica Acta*, 51(8-9), 1664–1672. https://doi.org/10.1016/j.electacta.2005.02.148.

[71] Sambare, A. A., Pawar, R., & Shirsat, M. (2023). A DFT investigation on transition metal (Co, Cr, Cu, Mn, Mo and Nb)-doped bismuth ferrite oxide (BiFeO3) for CO gas adsorption. *Theoretical Chemistry Accounts*, 142(7). https://doi.org/10.1007/s00214-023-03000-0.

[72] Sambare, A.A., Datta, K.P., Shirsat, M.D.et al (2022). Adsorption of gas molecules (CO, CO_2, NO_2, NO, and CH_4) on undoped and Ag-doped bismuth ferrite oxide (BFO) by DFT investigation. *Journal of Materials Research,* 37, 4296–4311. https://doi.org/10.1557/s43578-022-00800-1

[73] Sambare, A. A., & Pawar, R. (2024). Enhanced gas sensing performance of Ag-Doped BiFeO3 microspheres synthesized via flash auto combustion technology. *Current Chemistry Letters*, 13(2), 367–376. https://doi.org/10.5267/j.ccl.2023.10.008.

[74] Sambare, A., Pawar, R., & Shirsat, M. (2024). DFT + U +V Investigation on adsorption of gas molecules (CO, SO_2, NO, and NO_2) on Ni doped bismuth ferrite oxide (010). *Key Engineering Materials*, 980, 41–48. https://doi.org/10.4028/p-90hgo8